CrossMark

Influence of Rainfall, Model Parameters and Routing Methods on Stormwater Modelling

Yongwei Gong[1] · Xiaoning Li[2] · Dandan Zhai[3] · Dingkun Yin[1] ·
Ruining Song[1] · Junqi Li[1] · Xing Fang[2,4] · Donghai Yuan[1]

Abstract Quantification of the uncertainty associated with stormwater models should be analyzed before using modelling results to make decisions on urban stormwater control and management programs. In this study, the InfoWorks Integrated Catchment Modelling (ICM) rainfall-runoff model was used to simulate hydrographs at the outfall of a catchment (drainage area 8.3 ha, with 95% pervious areas) in Shenzhen, China. The model was calibrated and validated for two rainfall events with Nash-Sutcliffe efficiency >0.81. The influence of rainfall, model parameters and routing methods on outflow hydrograph of the catchment was systematically studied. The influence of rainfall was analyzed using generated rainfall distributions with random errors and systematic errors (± 30% offsets). Random errors had less influence than systematic errors on peak flow and runoff volume, especially for two rainfall events with larger depths and longer durations. The Monte Carlo simulations using 500 parameter sets were used to verify the equifinality of the nine model parameters and determine the prediction uncertainty. Most of the monitored flows were within the uncertainty range. The influence of two routing methods from rainfall excess to hydrograph was studied. The InfoWorks ICM model incorporating double quasilinear reservoir routing was found to have a larger effect on the simulated hydrographs for rainfall events having larger depths and longer durations than using the U.S. EPA's Storm Water Management Model nonlinear reservoir routing method did.

✉ Junqi Li
  li6700@163.com

1   Key Laboratory of Urban System and Water Environment, Ministry of Education, Beijing University of Civil Engineering and Architecture, Beijing, People's Republic of China

2   Department of Civil Engineering, Auburn University, Auburn, AL, USA

3   China Water Environment Group Limited, Beijing, People's Republic of China

4   Beijing Cooperative Innovation Research Centre on Architectural Energy Saving and Emission Reduction, Beijing University of Civil Engineering and Architecture, Beijing, People's Republic of China

⧍ Springer

1 Introduction

In recent years, stormwater models that are used as design, optimization and evaluation tools play a critical role in urban stormwater drainage management (Beck et al. 2017; Massoudieh et al. 2017). Several commonly-used comprehensive urban stormwater simulation models include the United States (U.S.) Environmental Protection Agency (EPA) Storm Water Management Model (SWMM) (Baffaut and Delleur 1989), InfoWorks Integrated Catchment Modeling (ICM) (Wallingford 2015), and the Danish Hydraulic Institute MIKE model (Doulgeris et al. 2012). However, model predictions are subject to uncertainty for various reasons and total elimination of uncertainty is not possible (Harremoës 2003). Therefore, quantifying the uncertainty of model prediction is important in order to understand the behavior of a model, assess the level of reliability of the model results and provide a robust basis for their practical application. The uncertainty of model prediction is due to model inputs, parameter selection and calibration based on limited rainfall events, model structure, and approximation of natural processes for a model (Freni et al. 2009; Harmel and Smith 2007; Miguntanna et al. 2010).

Interference factors such as evaporation, outsplash, wind and rain-gauge height above ground may all affect the accuracy of rainfall measurement. Nandakumar and Mein (1997) also determined that 10% deviation of evaporation resulted in 10% deviation of runoff; however, 10% deviation of rainfall resulted in 35% deviation of runoff when using the Monash model.

The influence of model parameters on simulation results should be assessed before the simulation results are used in the decision-making process. The Generalized Likelihood Uncertainty Estimation (GLUE) method (Beven and Binley 1992), Bayesian approach (Bayes and Price 1763), Markov Chain Monte Carlo (MCMC) method (Kao and Hong 1996) and first-order error analysis (Melching and Yoon 1996) are commonly used to study the prediction uncertainty resulted from model parameter selection. In this study, Monte Carlo (MC) simulations were conducted to examine the equifinality and the influence or uncertainty of model parameters on an outflow hydrograph. The equifinality (Beven and Freer 2001) means different parameter sets may produce similar simulation results.

For runoff modeling in hydrology, model structural deficits arise primarily from process misspecifications, insufficient spatial resolution, oversimplified empirical equations, and numerical errors. The model structure for hydrological models depends on the selection of the perceptual model and the conceptual/physical model. The influence of the model structure on the model performance for catchment runoff, including high- and low-flow conditions, was investigated by Butts et al. (2004) using an ensemble of two hydrological models (MIKE 11 and MIKE SHE) with different spatial resolutions and process descriptions.

In this paper, we systematically analyzed the influence of rainfall, model parameters and catchment routing methods on outflow prediction using InfoWorks ICM (Digman et al. 2014; Wallingford 2015). The aim of this study was to quantify uncertainties of outflow prediction from this integrated stormwater model for decision-making in comprehensive water resources management of the study catchment when the model was calibrated and validated using available observed data from two rainfall events.

2 Material and Methods

2.1 Study Area and Data

The study area is one of the 11 catchments located in the New District Park, an ecological municipal park of 56 ha located in the Guang-Ming New District, Shenzhen, China. The catchment has a drainage area of 8.3 ha, 95% of which is pervious (green space). The mean annual temperature of the study region is 22 °C and the mean annual precipitation is 1837 mm, most of which falls from April to September.

The rainfall data were recorded by a Watchdog 3554WD rain gauge in one-minute intervals. Discharges were measured by a FL900 flowmeter installed in the catchment outfall (Fig. 1). Six rainfall events used for the study were monitored in 2013 and observed outfall discharges were available for only two rainfall events: May 19 and September 14, 2013. Data from these two events were used to calibrate and validate the InfoWorks ICM model, respectively. The rainfall data for the other four events were used in the uncertainty analysis. Severe tropical storms on August 17 and 30, 2013 produced rainfall depths of more than 90 mm. The maximum 1-min rainfall intensities for all six events were similar (1.3–1.8 mm/ min). The rainfall event on May 19, 2013 had the highest average rainfall intensity (1.1 mm/ min) and the shortest duration (18 min). The two rainfall events for model calibration and validation had similar and relatively small rainfall depths (19.9 mm and 18.3 mm) but quite different durations (18 min and 70 min). The six rainfall events used in the study had durations
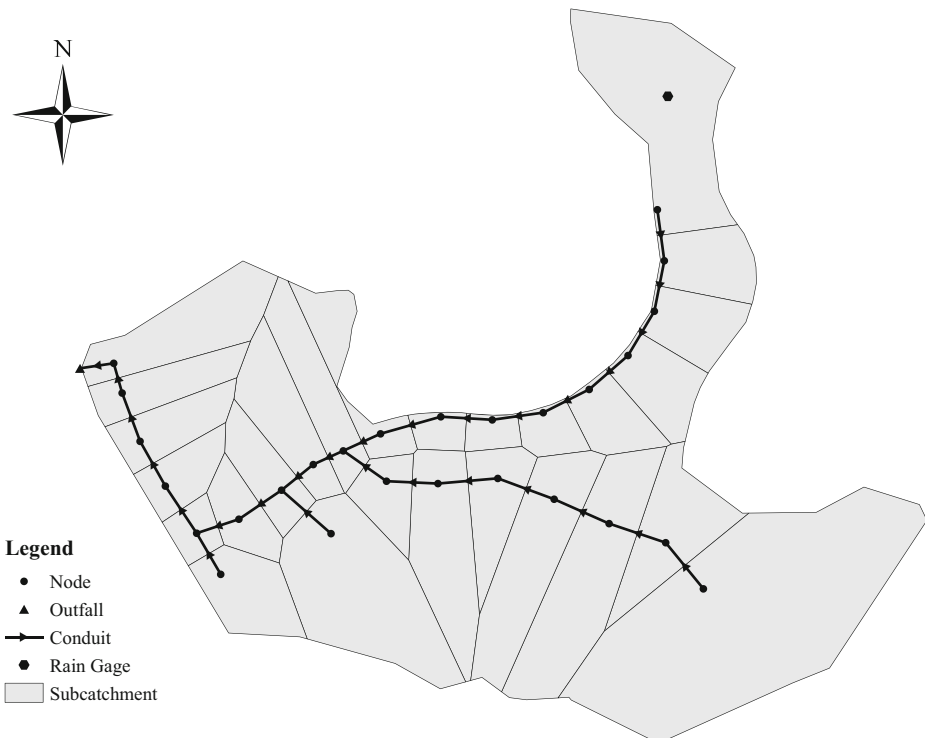

Fig. 1 Subdivision of the catchment based on the manholes as nodes

from 18 min to 344 min and depths from 18.3 to 139.9 mm. All these events allowed the study to identify model uncertainties for a broad range of rainfall depth and duration events and to understand whether or not the model works for heavy rainfall events and for longer duration events after the calibration and validation.

2.2 Model Description

InfoWorks ICM incorporates the hydraulics and hydrology of natural watersheds and man-made environments into a single integrated model. A rainfall–runoff model determines rainfall losses, including initial losses, infiltration and evaporation. It then transfers the rainfall excess into a runoff hydrograph (Viessman and Lewis 2003). Initial losses may be specified either as absolute losses or losses as function of slope in InfoWorks ICM. The absolute loss method was used and allows the modeler to input a constant initial rainfall loss (mm).

The InfoWorks ICM provides seven alternative runoff volume models—methods for determining rainfall excess after initial rainfall losses (Wallingford 2015). In this study, the fixed percentage model was used for impervious areas such as roofs and roads, and the Horton model was used for pervious areas.

Several runoff routing models are available in InfoWorks ICM for simulating the storage and transport of rainfall excess by surface drainage network before entering into the underground stormwater pipelines in an urban catchment: (i) the double quasilinear reservoir (DQLR) model, (ii) the SWMM nonlinear reservoir routing model, (iii) the Wallingford runoff routing model, and (iv) the unit hydrograph model (Viessman and Lewis 2003). Both kinematic- and dynamic-wave routing methods are available for the flow routing in stormwater pipelines (Wallingford 2015).

2.3 Model Setup, Calibration and Validation

In this study, manholes were considered as model nodes linking underground stormwater pipes. The Thiessen polygon tool of InfoWorks ICM was used to automatically divide the catchment into 27 sub-catchments (Fig. 1). The sub-catchment data includes drainage area, width, slope, and percent of impervious areas. The 27 sub-catchment areas range from 0.06 to 1.61 ha, the widths from 14.3 to 71.6 m, and the land slopes from 0 to 7%. The model also requires meteorological data, soil infiltration capability of pervious areas and underground stormwater pipelines information. Only one set of model parameters was used for all 27 sub-catchments with similar land use and soil conditions. The Nash–Sutcliffe efficiency (NSE) index (Nash and Sutcliffe 1970) was chosen to evaluate the simulation results for model calibration and validation.

2.4 Methods for Uncertainty Analysis

The InfoWorks ICM model of the catchment (Fig. 1) after calibration and validation was then used to systematically study the influence of rainfall, model parameters and routing methods on outflow hydrographs.

2.4.1 Uncertainty from Rainfall

Rainfall data is a greater source of uncertainty in the runoff simulation results than evaporation, air temperature or other meteorological data (Moradkhani and Sorooshian 2009). The rainfall

inputs may have random errors and systematic errors. The random errors of rainfall were modeled using ten rainfall distributions with random errors generated from

$$I_i^* = I_i(1-\alpha) \tag{1}$$

where I_i^* is the rainfall including the random error for the time step i; I_i is the measured rainfall intensity; αI_i is the random error; and the coefficient α is selected from a uniform distribution in the range of $(-0.5, 0.5)$ (Carpenter and Georgakakos 2004) using a random number generator.

Systematic errors in the rainfall measurements are mainly caused by the accuracy of the rain gauges, and also whether the rainfall measured at a point location represents the rainfall in the entire catchment. Molini et al. (2001) reported average absolute errors of measured rainfall to be in the order of 10–30%. Therefore, in this study the systematic error in rainfall data was assumed to be ±30% offset of the observed rainfall. The model uncertainty from rainfall inputs on outflow prediction was first investigated using above generated rainfall time series with random errors or systematic errors.

2.4.2 Uncertainty from Model Parameters

Nine model parameters (Table 1) were chosen for determining the model uncertainty and their significance on simulated outfall hydrographs using the Monte Carlo method. Manning's n values for underground conduits, impervious and pervious surfaces are 0.11–0.015, 0.011–0.033 and 0.1–0.8; the impervious and pervious depressions are 0.2–10 mm and 2–12 mm; the runoff coefficient is 0.7–0.9; the initial infiltration rate, equilibrium infiltration rate, and decay constant are 70–200 mm/h, 2–30 mm/h, and 2–7 h^{-1}, respectively, based on recommendations for InfoWorks ICM. Due to the lack of information regarding the distributions of the parameters, a uniform distribution was adopted for sampling each parameter.

The NSE objective function and NSE threshold of 0.7 were selected and used to evaluate the acceptability threshold of the model parameter values (Freni et al. 2008). The NSE was calculated from simulated and observed flows for the rainfall event on May 19, 2013, and was used to assess and verify the equifinality of the model parameters.

Table 1 Calibrated model parameters and statistical summary and the 90% parameter intervals of behavioral model parameters (NSE ≥ 0.7)

Parameters	Calibrated	Min.	Maxi.	Average	Deviation	5%, 95% intervals
n-Conduit	0.013	0.0110	0.0150	0.0130	0.0011	0.0114, 0.0148
n_{Imper} [a]	0.013	0.0111	0.0330	0.0222	0.0063	0.0124, 0.0318
n_{Per}	0.200	0.1022	0.7993	0.4564	0.2012	0.1416, 0.7668
D_{Imper} (mm)	2.0	0.20	8.54	3.80	2.16	0.69, 7.79
D_{Per} (mm)	10.0	2.01	11.98	8.04	2.69	3.41, 11.74
C [b]	0.75	0.701	0.900	0.799	0.057	0.711, 0.889
f_o (mm/h) [c]	76.0	70.41	199.90	135.96	36.99	78.02, 192.86
f_c (mm/h)	2.5	2.06	29.94	15.85	8.03	3.37, 28.38
k (hr^{-1})	2.0	2.02	6.99	4.48	1.46	2.24, 6.77

[a] for the SWMM nonlinear reservoir routing model, the subscript "Imper" stands for impervious, "Per" for pervious surface

[b] for the fixed percentage method

[c] for Horton's equation

Latin Hypercube Sampling (LHS) was used to sample 500 sets of the nine model parameters (Table 1). The LHS method, proposed by McKay et al. (2000) as an improvement on Monte Carlo sampling (Hastings 1970) facilitates access to a wider range of parameter values. Since modelers can readily grasp the overall modeled results, it is widely used in model parameter uncertainty analysis.

The model was run for each set of model parameters and the likelihood measure was calculated using the modeled and measured flow at the outfall. If the likelihood measure exceeded the NSE threshold, the simulation and the parameter set were considered to be 'behavioral' and were saved for the following analysis steps; if not, they were discarded as 'non-behavioral'. For the behavioral parameter sets, the probability density distribution and cumulative probability density distribution were obtained for each parameter in order to quantify model parameter uncertainty.

The 5% and 95% percentiles (Table 1) of the behavioral parameter set were assumed to represent the uncertainty bands in this study (Dotto et al. 2012); that is, the 'true' value of each model parameter should lie within that percentile region. The 5% and 95% percentiles of the simulated flows in each output time step were determined to give the 90% prediction interval of simulated flow, quantifying the uncertainty due to those particular model parameters.

2.4.3 Uncertainty from Routing Methods

This study also focused on the uncertainty of the simulated runoff hydrographs for the catchment routing methods for transforming the rainfall excess to the hydrograph. Two model scenarios (A and B) were studied. The scenario A was used throughout the study for model calibration and validation, and for sensitivity analysis of rainfall and model parameters. The overland flow routing in SWMM solves the Manning formula and the continuity equation, and it is a hydraulic—not hydrological—routing method. The overland flow routing in SWMM as an option under InfoWorks ICM was classified as a nonlinear reservoir routing method used in scenario A.

For the scenario B, the overland flow routing model was the UK Wallingford Procedure (Wallingford 1981). The DQLR method was applied in series (Eq. (2)) for each surface type (two impervious areas and one pervious area) with the same storage–outflow relationship for each hypothetical reservoir: $S = \lambda Q$, where S is the storage and Q is the outflow of the reservoir, and λ is a linear reservoir routing constant that is inversely proportional to the running ten-minute average rainfall intensity (i_{10}); therefore, λ is not a constant, but varies with rainfall and thus leads to a quasilinear reservoir model (Price and Vojinovic 2011).

$$Q(t) + 2\lambda \frac{dQ(t)}{dt} + \lambda^2 \frac{d^2 Q(t)}{dt^2} = i_n \qquad (2)$$

$$\lambda = c i_*^{-0.39} \quad \lambda i_* = (1 + i_{10})/2 \qquad (3)$$

where $Q(t)$ is the outflow of the two reservoirs as a function of time t; i_n is the net rainfall intensity multiplied by catchment area; and c is an empirical coefficient, which is a function of the catchment area and slope (Wallingford 1981). In the UK Wallingford method, the user specifies rainfall, catchment slope and area, and a runoff routing parameter for impervious areas and another for pervious areas. In this study, the runoff routing parameter was set to be 1, 1 and 4 for buildings, roads and green space, respectively, as recommended by Wallingford (1981).

3 Results and Discussion

3.1 Calibration and Validation Results

The simulated hydrographs at the outfall for the model calibration and validation compared well with observed data (Fig. 2). The rainfall depth on May 19, 2013 for the model calibration, was only 1.6 mm more than the rainfall depth on September 14, 2013 for the model validation. But the May event produced a much greater flow than occurred in the September event. Its shorter duration (18 min.) and higher intensity (up to 1.8 mm/min) produced a simulated peak discharge of 86.9 L/s. The longer-duration rainfall (1 h 10 min.) event on September 14 resulted in a simulated peak discharge of only 9.9 L/s. The NSE values for model calibration and validation were 0.92 and 0.81, respectively, which indicated satisfactory performance of the model. The manually calibrated model parameters are summarized in Table 1.
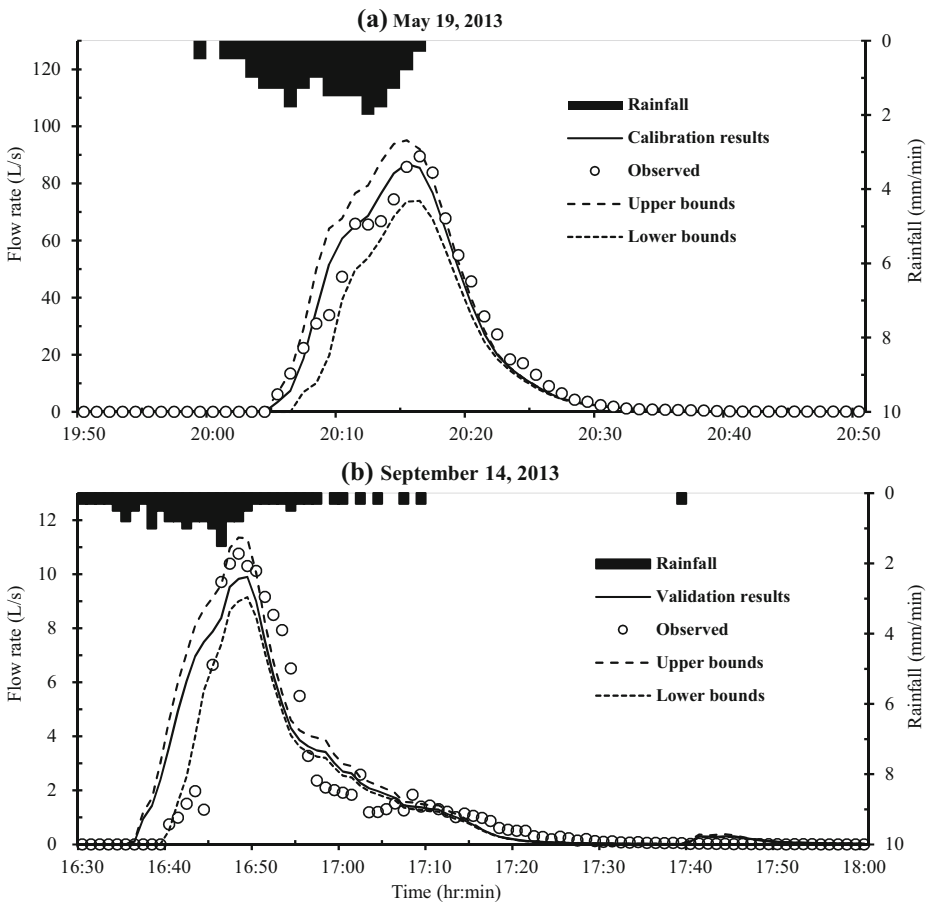

Fig. 2 Simulated and observed hydrographs (different scales on *x*- and *y*-axes) including uncertainty bounds of simulated flow defined by 90% prediction intervals with rainfall hyetographs on (**a**) May 19, 2013, (**b**) September 14, 2013

3.2 Uncertainty Analysis of Rainfall

3.2.1 Random Rainfall Errors

For random error analysis, the first two events (April 25 and July 10, 2013) had relatively small rainfall depths, and the last two events (August 17 and 30, 2013) had much larger rainfall depths (Table 2). The statistical characteristics of the 10 rainfall distributions with random errors summarized in Table 2 encompass adequate ranges of rainfall depth and peak rainfall intensity for each event. The rainfall depth variation, taking the random errors into account, was about 8–11%, but the variation in peak intensity was much larger (40–82%).

The InfoWorks ICM model was run for all 40 rainfall hyetographs using the calibrated model parameters (Table 1). The simulated hydrographs for the four observed rainfall events are shown in Fig. 3 together with maximum and minimum envelope curves for the discharges of 10 simulated hydrographs from rainfall distributions with random errors. In addition to the envelope curves, the uncertainty of simulated flow at the outlet on rainfall with the random errors was further quantified by the peak discharge (Q_p) variation, the average discharge variation and the variation in runoff volume (V_{runoff} in m^3) (Table 3). The average of all discharge variations for flows ≥5.0 L/s on the hydrograph was calculated for each event to quantify the overall uncertainty or variation due to random errors in the simulated outflow hydrograph. The calculated variations in Q_p and averages of discharge variations ranged from 25.5% to 45.7% and from 29.6% to 41.7%, respectively (Table 3), because the peak intensity variations were 40% or more. The runoff volume in m^3 was calculated for each event by numerical integration. The calculated variations in V_{runoff} ranged from 10.5% to 22.8%; these values were similar to the rainfall depth range values for the other events except for the 8/17/2013 event.

3.2.2 Systematic Rainfall Errors

The four rainfall events were also used to quantify the uncertainty of simulated flow caused by systematic errors of rainfall. Fig. 3 also shows the simulated hydrographs from rainfall

Table 2 Characteristics of observed and ten rainfall distributions with random errors generated from four observed rainfall events

Parameters \ Date	4/25/2013	7/10/2013	8/17/2013	8/30/2013
Observed rainfall duration	6:43	1:05	4:56	5:44
Observed rainfall T_{peak}[a]	0:38	0:05	2:14 & 3:00	1:26
Observed rainfall depth (mm)	40.9	27.7	93.6	139.9
Maximum rainfall depth (mm)	42.6	28.8	98.4	145.9
Minimum rainfall depth (mm)	38.1	26.2	90.3	134.9
Rainfall depth variation[b]	11.0%	9.4%	8.7%	7.9%
Average rainfall depth (mm)	40.48	27.62	94.20	139.81
Standard deviation (mm)	1.64	0.99	2.54	3.84
Coefficient of Variation[b]	0.040	0.036	0.027	0.030
Observed i_{peak} (mm/min)[c]	1.50	1.30	1.80	1.80
Maximum i_{peak}(mm/min)	2.10	1.95	2.52	2.7
Minimum i_{peak}(mm/min)	1.43	0.88	1.80	1.80
i_{peak} variation[b]	44.7%	82.3%	40.0%	50.0%

[a] T_{peak} is time (hr:min) of peak rainfall from the beginning of the rainfall event

[b] variation (%) = (Maximum - Minimum)/Observed event quantity

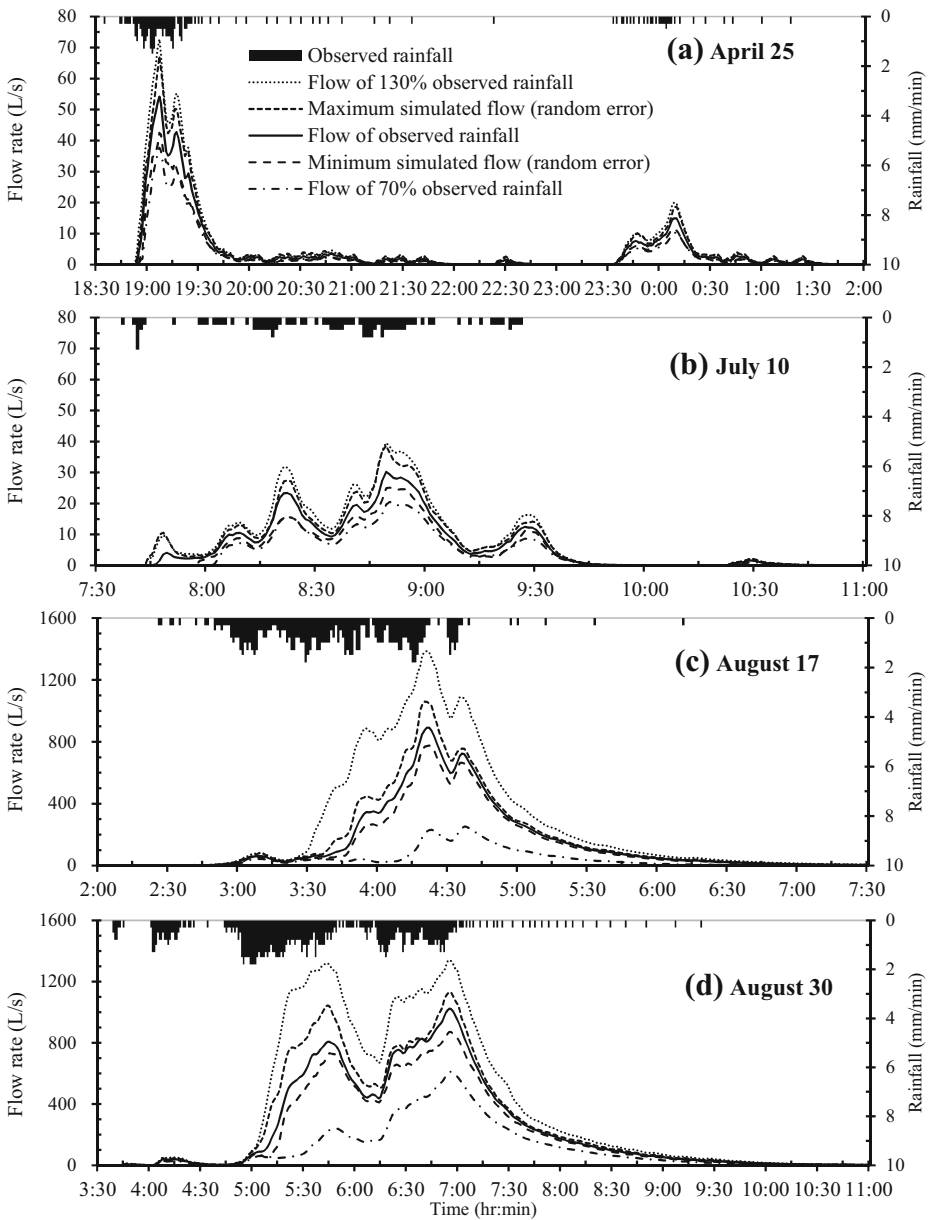[c] i_{peak} stands for peak rainfall intensity

Fig. 3 Simulated hydrographs for observed rainfalls, maximum and minimum envelope curves for simulated discharges using 10 rainfall inputs with random errors and using rainfalls with ±30% systematic errors for four rainfall events in 2013: (**a**) April 25, (**b**) July 10, (**c**) August 17, and (**d**) August 30. Different scales are used on the *x*- and *y*-axes for the four events

distributions having ±30% systematic errors. The constant ±30% offsets were applied to all time intervals on the observed hyetographs. The outfall hydrographs show similar variations with time for all three rainfall distributions because the hyetographs with systematic errors only had the offsets but no time shift, and the same model parameters were used for all simulations.

Table 3 Statistical summary of simulated hydrographs using ten rainfall hyetographs with random errors for four observed rainfall events

Parameters \ Date	4/25/2013	7/10/2013	8/17/2013	8/30/2013
Q_p (L/s, observed rainfall)	54.17	30.23	891.24	1023.21
Maximum Q_p (L/s)	67.24	38.69	1060.39	1131.97
Minimum Q_p (L/s)	42. 51	25.98	776.16	871.12
Maximum Q_p variation[a]	45.7%	42.0%	31.9%	25.5%
Average of discharge varation[b]	41.7%	36.5%	29.6%	30.1%
V_{runoff} (m³, observed rainfall)	120.44	80.3	2982.7	6478.72
Maximum V_{runoff} (m³)	125.59	83.9	3394.4	6973.46
Minimum V_{runoff} (m³)	111.64	75.4	2713.0	6048.89
Maximum V_{runoff} variation[a]	11.6%	10.5%	22.8%	14.3%

[a] variation = (Maximum - Minimum)/Observed quantity

[b] Discharge variation = $[Q_{max}(t) - Q_{min}(t)]/Q_{obs}(t)$, where $Q_{max}(t)$, $Q_{min}(t)$, $Q_{obs}(t)$ are simulated discharges at different time of hydrographs plotted on Fig. 3

The starting time of the runoff hydrographs for 70% observed rainfalls was 1–8 min later than the simulated hydrographs for the observed rainfalls; for 130% observed rainfalls, the starting time of the runoff hydrographs was 2–11 min earlier than for the simulated hydrographs for the observed rainfalls (Fig. 3). No differences were seen in the peak times for any of the three rainfall scenarios, which implied that the systematic errors in the rainfall measurement had some influence on the runoff generation time, since the initial rainfall losses were identical for all three rainfall hyetographs.

The hydrographs simulated from observed rainfalls, the variations of the peak flow Q_p and the total runoff volume V_{runoff} between 130% and 70% observed rainfalls were compared. The variations of Q_p and V_{runoff} (mm, normalized by area) were similar to the rainfall systematic errors (± 30%) for the two rainfall events with relatively small rainfall depths (April 25 and July 10, 2013). The rainfall event on August 17, 2013 was comprised of a continuous and relatively high rainfall intensity for 1.5 h, with a single large peak discharge (Fig. 3). The variations of Q_p and V_{runoff} are −74.1 to 55.7% and −73.0 to 76.2% for the 70% and 130% rainfalls, respectively, which were up to 2.5 times larger than the rainfall random errors. The overall variations for Q_p and V_{runoff} due to systematic errors were up to 129.8% and 149.2%, respectively. The rainfall event on August 30, 2013 consisted of rainfall over two separate time periods of approximately one hour in length with a half-hour time period of lower intensity between the two. This resulted in two similar large peak discharges (Fig. 3), and the variations of Q_p and V_{runoff} were −40.3 to 31.1% and −52.8 to 53.1% for 70% and 130% rainfalls, respectively.

Rainfall loss of pervious areas was determined by the Horton infiltration method, which gave a high infiltration capacity at time $t = 0$ ($f_o = 76$ mm/h) and decreased rapidly with time in the early hours of the rainfall event ($k = 2$ h⁻¹, Table 1). When the total rainfall depth was small and of short duration (events April 25 and July 10, 2013), the rainfall loss showed a large increase with increasing rainfall depth. For example, in the April 25, 2013 event the loss increased by 85.5% (from 27.6 mm to 51.3 mm) when the rainfall increased by 60%. This effect is seen when the Horton infiltration capacity exceeds the rainfall intensity for most of the rainfall event.

For the two events with larger rainfall depths and of longer durations (August 17 and 30, 2013), the rainfall loss was <3.2% increase for a 30% rainfall increase. This occurs when the Horton infiltration capacity is close to the equilibrium infiltration rate ($f_c = 2.5$ mm/h, Table 1) and smaller than the rainfall intensity late in the rainfall event. Therefore, the peak discharge and runoff volume variations are different for rainfall events of different depths and intensities

from ±30% rainfall systematic errors. The rainfall systematic error could cause great uncertainty of simulation results for the rainfall event with large depth and long duration.

3.3 Analysis of Model Parameter Uncertainty

3.3.1 Equifinality for Different Parameters

Parameter sets and corresponding NSE values for the Monte Carlo simulations using 500 parameter sets are shown in Fig. 4 for nine model parameters (Table 1). Although the values of the parameters in each set were dissimilar, it was found in 440 of the 500 parameter sets that the objective function values exceeded 0.7 (Fig. 3). From this it was inferred that the equifinality principle was applicable to the model parameters selected for the catchment. Traditional manual calibration methods of establishing calibrated model parameters had certain limitations (Table 1). Fig. 4a shows that the depression storage in impervious areas was strongly correlated with NSE, but the other parameters were not; this suggests that parameter identification or selection for InfoWorks ICM has a high level of uncertainty. Zhao et al. (2009), in a study using SWMM for a hydrological uncertainty analysis in Macao, also concluded that depression storage in impervious areas was a sensitive parameter for simulated
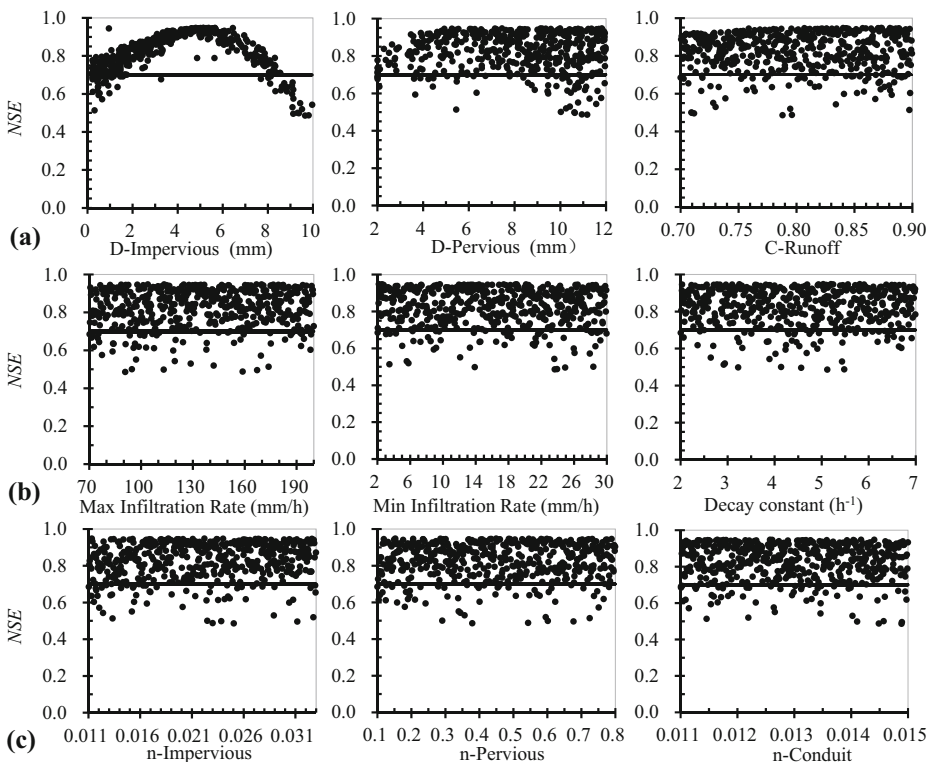

Fig. 4 Scatter plots of NSE: (**a**) likelihood for initial loss parameters and runoff coefficient used in InfoWorks ICM model; (**b**) likelihood for Horton infiltration parameters for green spaces used in InfoWorks ICM model; (**c**) likelihood for Manning roughness coefficient used in InfoWorks ICM model

hydrographs. Using Monte Carlo simulations, parameter sets, but not one most optimized parameter set, were identified for the InfoWorks ICM model of the study catchment.

The posterior probability distribution of depression storage D (mm) for impervious areas was developed (Song 2014) and similar to a normal distribution with negative or left skewness, whereas D for pervious areas had a trapezoidal distribution with the higher probability on the higher D values or right skewness. These were both unlike their prior distributions, which were uniform. Parameter uncertainty and identification were strongly related to their posterior distribution, which is consistent with finding in a previous study (Sun and Yeh 1990). When the posterior probability distribution differs markedly from the prior distribution, the model performance is more sensitive to the parameter, and thus better-optimized parameter values or ranges may be identified. The posterior distributions of the other parameters were similar to their prior distributions (Song 2014); in such cases, the model is not sensitive to those parameters and a lesser uncertainty is attached to their selection. Therefore, from the above discussion, the selection of parameter D for impervious and pervious areas had a stronger recognition and identification value than other parameters. For example, the rainfall depth on May 19, 2013 was relatively small, and depression storage had a more significant effect on model output than for higher rainfalls.

3.3.2 Prediction Uncertainty from Model Parameters

The Monte Carlo simulations identified 440 sets of behavioral parameters for the InfoWorks ICM model when an NSE threshold of 0.7 was adopted. The statistical summary and 90% parameter intervals (95% and 5% percentiles) of the nine model parameters are given in Table 1. Most of the calibrated model parameters are within the range defining behavioral parameters (Table 1). The calibrated infiltration parameters (f_o and f_c) had relatively low values (outside the 90% parameter intervals) when only two rainfall events were used for model calibration and validation (Fig. 2).

The likelihood functions for different NSE values (Fig. 4) were determined for the rainfall event on May 19, 2013 using observed hydrograph data. The 440 sets of behavioral parameters identified from that rainfall event were applied to the rainfall event of September 14, 2013. The 90% prediction intervals (upper and lower bounds) of flow at the outlet are plotted in Fig. 2 to show the bounds of uncertainty for the simulated runoff on those dates.

The observed peak flow on May 19 was 89.5 L/s, slightly larger than the upper bound of the predicted peak (85.4 L/s, Fig. 2). The observed peak flow on September 14 was 10.8 L/s, slightly smaller than the upper bound of the predicted peak (11.4 L/s). The most of observed flows are contained within the uncertainty range (Fig. 2).

3.3.3 Uncertainty Analysis of Routing Methods

When observed rainfall hyetographs were used, the simulated outfall hydrographs for the four rainfall events (Fig. 5) show similar variations with time in two different scenarios. These scenarios examine the uncertainty of catchment routing methods, since hydrograph shapes are predominantly determined by rainfall distributions. For the scenario B with the InfoWorks DQLR routing model, the simulated hydrographs for the two smaller rainfall events (April 25 and July 10, 2013) showed 3.0–4.7% attenuation in peak discharge and one minute of delay in the time of the peak. For the two larger rainfall events of longer durations (August 17 and 30, 2013), the simulated hydrographs for the scenario B showed higher peak discharges and larger runoff volumes, but no
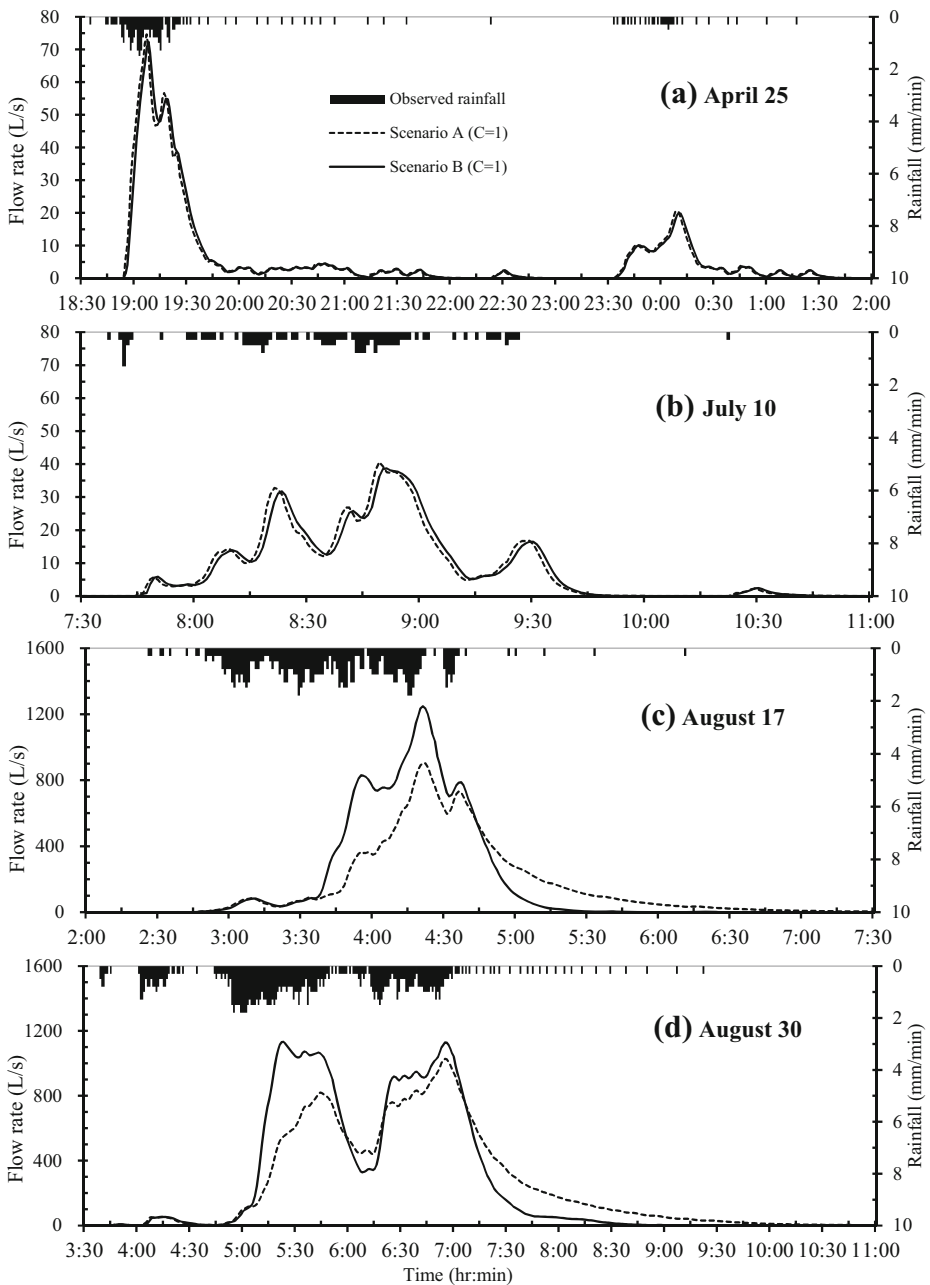
Fig. 5 Simulated hydrographs at the outfall for model structure scenarios A and B for four rainfall events in 2013: (**a**) April 25, (**b**) July 10, (**c**) August 17, and (**d**) August 30. Different scales in *x*- and *y*-axes are used for the four events

delay or earlier peak discharge time. The simulated peak discharges were 38.3% and 10.3% larger than those in the scenario A with the DQLR routing model, and simulated runoff volumes were 13.7% and 4.4% larger. For the DQLR routing model, the routing coefficient (Eq. (3)) is smaller for

higher-intensity rainfall, which results in higher discharge (less attenuation) and smaller ponding depth on the surface. The smaller ponding depth reduces the actual infiltration rate when the Horton infiltration capacity exceeds the gross rainfall intensity. It seems that the storage constant for the DQLR routing in InfoWorks ICM is smaller than the one in SWMM using the Manning coefficient when the rainfall intensity is large.

4 Summary and Conclusions

This study focused on simulating discharge at the outfall from a small watershed (8.3 ha) with a 95% of pervious area using InfoWorks ICM software. Summaries and main conclusions of the study are given below:

(1) Model uncertainty from rainfall was studied using perturbed rainfall data with random and systematic errors. Ten rainfall distributions were generated with random errors of 8–11% in rainfall depths and 40–82% in peak rainfall intensity, resulting in 11–23% variations in total runoff volume V_{runoff} and 26–46% variations in peak discharge Q_p. Assumed systematic errors having ±30% offsets form observed rainfall distribution resulted in similar variations (approximately ±30%) in V_{runoff} and Q_p for the two events with relatively smaller depths (<41 mm) and shorter durations, but for the two events with larger rainfall depths (>93 mm) and longer durations, variations in V_{runoff} and Q_p are up to 2.5 times larger than the rainfall random errors. The overall variations for Q_p and V_{runoff} due to the ±30% systematic errors were up to 129.8% and 149.2%.

(2) Monte Carlo simulations using 500 parameter sets developed from the LHS were conducted to study the uncertainty of simulated outflow from nine model parameters of InfoWorks ICM. The "Equifinality" phenomenon was found to exist in model parameters of InfoWorks ICM. Most of the monitored flows for the two events (May 19 and September 14, 2013) are contained in the simulated uncertainty range.

(3) For the uncertainty of the routing methods in the InfoWorks ICM model, the hydrographs simulated by the DQLR routing model for the two events with small rainfall depths are almost the same as those from ICM's SWMM nonlinear reservoir routing model; however, the DQLR simulated hydrographs for the two rainfall events with larger depths and longer durations had higher peak discharges, larger runoff volumes, and no delayed or early peak time. Contributors to these differences included changes in the storage constant with greater rainfall intensity, which further impacts on the actual filtration rate when the Horton infiltration capacity is larger than the rainfall intensity.

The uncertainty analyses of rainfall, model parameters and routing methods from excess to hydrograph in this study were for a catchment with 95% pervious areas and limited rainfall events; therefore, some results may not be readily generalized for catchments in other regions with different catchment and rainfall characteristics.

References

Baffaut C, Delleur J (1989) Expert system for calibrating SWMM. J Water Resour Plan Manag 115:278–298

Bayes M, Price M (1763) An essay towards solving a problem in the doctrine of chances. Philos Trans 53(1683-1775):370–418

Beck NG, Conley G, Kanner L, Mathias M (2017) An urban runoff model designed to inform stormwater management decisions. J Environ Manag 193:257–269. https://doi.org/10.1016/j.jenvman.2017.02.007

Beven K, Binley A (1992) The future of distributed models: model calibration and uncertainty prediction. Hydrol Process 6:279–298

Beven K, Freer J (2001) Equifinality, data assimilation, and uncertainty estimation in mechanistic modelling of complex environmental systems using the GLUE methodology. J Hydrol 249:11–29

Butts MB, Payne JT, Kristensen M, Madsen H (2004) An evaluation of the impact of model structure on hydrological modelling uncertainty for streamflow simulation. J Hydrol 298:242–266

Carpenter TM, Georgakakos KP (2004) Impacts of parametric and radar rainfall uncertainty on the ensemble streamflow simulations of a distributed hydrologic model. J Hydrol 298:202–221

Digman CJ, Anderson N, Rhodes G, Balmforth DJ, Kenney S (2014) Realising the benefits of integrated urban drainage models. Proc Inst Civ Eng 167:30–37

Dotto CB et al (2012) Comparison of different uncertainty techniques in urban stormwater quantity and quality modelling. Water Res 46:2545–2558

Doulgeris C, Georgiou P, Papadimos D, Papamichail D (2012) Ecosystem approach to water resources management using the MIKE 11 modeling system in the Strymonas River and Lake Kerkini. J Environ Manag 94:132–143

Freni G, Mannina G, Viviani G (2008) Uncertainty in urban stormwater quality modelling: the effect of acceptability threshold in the GLUE methodology. Water Res 42:2061–2072

Freni G, Mannina G, Viviani G (2009) Urban runoff modelling uncertainty: comparison among Bayesian and pseudo-Bayesian methods. Environ Model Softw 24:1100–1111

Harmel RD, Smith PK (2007) Consideration of measurement uncertainty in the evaluation of goodness-of-fit in hydrologic and water quality modeling. J Hydrol 337:326–336

Harremoës P (2003) The need to account for uncertainty in public decision making related to technological change. Integr Assess 4:18–25

Hastings WK (1970) Monte Carlo sampling methods using Markov chains and their applications. Biometrika 57:97–109

Kao J-J, Hong H-J (1996) NPS model parameter uncertainty analysis for an off-stream reservoir. JAWRA Journal of the American Water Resources Association 32:1067–1079. https://doi.org/10.1111/j.1752-1688.1996.tb04074.x

Massoudieh A, Maghrebi M, Kamrani B, Nietch C, Tryby M, Aflaki S, Panguluri S (2017) A flexible modeling framework for hydraulic and water quality performance assessment of stormwater green infrastructure. Environ Model Softw 92:57–73. https://doi.org/10.1016/j.envsoft.2017.02.013

McKay MD, Beckman RJ, Conover WJ (2000) A comparison of three methods for selecting values of input variables in the analysis of output from a computer code. Technometrics 42:55–61

Melching CS, Yoon CG (1996) Key sources of uncertainty in QUAL2E model of Passaic River. J Water Resour Plan Manag 122:105–113

Miguntanna NS, Egodawatta P, Kokot S, Goonetilleke A (2010) Determination of a set of surrogate parameters to assess urban stormwater quality. Sci Total Environ 408:6251–6259

Molini A, La Barbera P, Lanza L, Stagi L (2001) Rainfall intermittency and the sampling error of tipping-bucket rain gauges. Physics and chemistry of the earth, part C: solar, terrestrial & Planet Sci 26:737–742

Moradkhani H, Sorooshian S (2009) General review of rainfall-runoff modeling: model calibration, data assimilation, and uncertainty analysis. In: Sorooshian S, Coppola E, Verdecchia M, Hsu K-L, Tomassetti B, Visconti G (eds) Hydrological modelling and the water cycle. Springer, Berlin, pp 1–24

Nandakumar N, Mein RG (1997) Uncertainty in rainfall—runoff model simulations and the implications for predicting the hydrologic effects of land-use change. J Hydrol 192:211–232

Nash JE, Sutcliffe JV (1970) River flow forecasting through conceptual models part I—A discussion of principles. J Hydrol 10:282–290

Price RK, Vojinovic Z (2011) Urban hydroinformatics: data, models, and decision support for integrated urban water management. International Water Association, London

Song R (2014) Uncertainty analysis of Stormwater modeling based on InfoWorks ICM model. Beijing University of Civil Engineering and Architecture, Beijing

Sun N, Yeh WWG (1990) Coupled inverse problems in groundwater modeling: 1. Sensitivity analysis and parameter identification. Water Resour Res 26:2507–2525

Viessman W, Lewis GL (2003) Introduction to hydrology, 5th edn. Pearson Education, Upper Saddle River

Wallingford (1981) Design and analysis of urban stormwater drainage - the Wallingford procedure. Department of Environment, National Water Council, UK

Wallingford (2015) InforWorks ICM Product Information - Overview. http://www.innovyze.com/products/infoworks_icm. Accessed Oct 28 2015

Zhao D, Wang H, Chen J, Wang H (2009) Parameters uncertainty analysis of urban rainfall-runoff simulation. Advances in Water Science (Chinese) 20:45–51